



Microwave absorption properties of $\text{Sr}_2\text{FeMoO}_6$ nanoparticles

L. Xi*, X.N. Shi, Z. Wang, Y.L. Zuo, J.H. Du

Key Laboratory for Magnetism and Magnetic Materials of Ministry of Education, Lanzhou University, Lanzhou 730000, PR China

ARTICLE INFO

Article history:

Received 26 November 2010

Received in revised form

11 March 2011

Accepted 11 March 2011

Available online 22 March 2011

Keywords:

Double perovskites

Microwave absorption properties

Magnetic properties

ABSTRACT

The microwave absorption properties of nanosized double perovskite $\text{Sr}_2\text{FeMoO}_6$ and epoxy resin composites were investigated in the frequency range of 2–18 GHz using the coaxial method. The $\text{Sr}_2\text{FeMoO}_6$ composites with an optimal 20 wt% epoxy resin showed a strong electromagnetic attenuation of -49.3 dB at 8.58 GHz with a matching thickness of 2.15 mm. Moreover the optimum absorption frequency at which the reflection loss is less than -20 dB, which corresponds to 99% reflection loss of the incident microwave, is from 5.7 to 13.2 GHz with the matching thickness ranging from 3.0 to 1.5 mm. The excellent microwave-absorption properties are a consequence of a proper electromagnetic match due to the existence of the insulating matrix of anti-site defects and anti-phase domains, which not only contribute to the dielectric loss but also to the reduced eddy current loss.

© 2011 Elsevier B.V. All rights reserved.

1. Introduction

Recently with the rapid development of information technology, serious electromagnetic interference pollution has triggered great interest in finding effective electromagnetic wave absorption materials with properties of wide and strong absorption frequency range, low density and high resistivity. Up to now several systems were investigated, such as nanoparticles of 3d-transition metals [1] and improved microwave absorption properties of their core/shell structures [2] due to the enhanced dielectric loss and the reduced eddy current loss by forming insulating shells. However, the process to obtain the core/shell structure is usually complicated. For application, it is essential to develop a material with good microwave absorption performance by a simple method.

Double perovskite $\text{Sr}_2\text{FeMoO}_6$ is a kind of spintronics material due to its half-metallic properties [3], which has large potential application in spintronic devices. Samples of $\text{Sr}_2\text{FeMoO}_6$ are usually prepared by the solid-state reaction or sol–gel method. However, it is prone to form anti-site defects (ASD), anti-phase domains (APD) and intrinsic disorder under certain conditions. The insulating matrix of the anti-phase defect and intrinsic disorder inside the $\text{Sr}_2\text{FeMoO}_6$ nanoparticles can reduce the eddy current loss and make it possible to be used as a microwave absorption material.

In this paper, $\text{Sr}_2\text{FeMoO}_6$ nanoparticles were fabricated by the sol–gel method at different sintering temperatures, which are the key factors to get the ideal half-metallic properties of $\text{Sr}_2\text{FeMoO}_6$ [4].

The microwave absorption properties of 80 wt% $\text{Sr}_2\text{FeMoO}_6$ nanoparticles and 20 wt% epoxy resin composites in the range of 2–18 GHz were determined by the coaxial method and a remarkable performance of electromagnetic wave absorption properties was reported.

2. Experiment details

$\text{Sr}_2\text{FeMoO}_6$ nanoparticles were prepared by the sol–gel method. Stoichiometric amounts of analytical grade $(\text{NH}_4)_6\text{Mo}_7\text{O}_{24} \cdot 4\text{H}_2\text{O}$, $\text{Sr}(\text{NO}_3)_2$ and $\text{Fe}(\text{NO}_3)_3 \cdot 9\text{H}_2\text{O}$ were used as starting materials. These compounds were dissolved in deionized water. Citric acid and glycol were added to the solutions with constant churning using a glass rod. The gels were dried at 110 °C for 2 days and then decomposed at 600 °C for 4 h in air in order to remove the elements of C, H and N. Later, the precursors were ground in an agate mortar and pelletized for further annealing at 900 °C for 6 h in air. The pelletized sample was annealed at different temperatures of 900, 950 and 1000 °C, for 6 h in air. Finally, the samples were annealed at the above-mentioned corresponding temperatures for 2.5 h in a H_2/Ar (3.7%/96.3%) reduction flow and named as S900, S950 and S1000, respectively.

Phase analysis was carried out using powder X-ray diffraction (XRD) technique with $\text{Cu K}\alpha$ radiation. Magnetic properties were measured using a Vibrating Sample Magnetometer at room temperature. The $\text{Sr}_2\text{FeMoO}_6$ sample was evenly mixed with epoxy at a mass ratio of 80% by ultrasound dispersion at 42 °C for 30 min. Toroidal $\text{Sr}_2\text{FeMoO}_6/\text{epoxy}$ samples with inner diameter of 3.04 mm, outer diameter of 7 mm and thickness of 1–2 mm were prepared to fit well with the coaxial sample holder for microwave measurements. The complex relative permeability

* Corresponding author.

E-mail address: xili@lzu.edu.cn (L. Xi).

($\mu_r = \mu' - j\mu''$) and permittivity ($\epsilon_r = \epsilon' - j\epsilon''$) of the composites were measured by the coaxial method on an Agilent E8363B vector network analyzer within the frequency range of 2–18 GHz.

3. Results and discussion

Fig. 1 shows the XRD patterns of the three samples. One can see that the diffraction peak positions of different samples are the same. All peaks in the diffraction patterns are consistent with those of the pure $\text{Sr}_2\text{FeMoO}_6$ phase [5] with tetragonal crystal structure. The Rietveld refinement method was used to analyse the occupation probability of Fe and Mo ions, since the anti-site defects were usually observed for double perovskites. Typical experimental, calculated XRD patterns and their difference of S950 are shown in Fig. 1(b). One can see that the calculated and the experimental XRD patterns are consistent with each other. The fitted reliable parameter R_{wp} values are 5.9%, 2.6% and 3.4% for S900, S950 and S1000 samples, respectively, indicating the reliable refinement results. The fitted anti-site defects decrease from 0.375 to 0.207 as the annealing temperature increases from 900 to 1000 °C, respectively. Thus, one can see a decreasing trend of the anti-site defects with the increase of annealing temperature, which is consistent with literature [6].

The average size of grains was calculated according to Scherrer's formula $D = k\lambda/B \cos \theta$, where k is a constant (0.89), λ is the wavelength of the X-ray, B is the width at the half-maximum of the peak (FWHM) and θ is the diffraction angle of the strongest diffraction peak. The $\text{Sr}_2\text{FeMoO}_6$ grain size is estimated to be about 42, 48 and 49 nm for S900, S950 and S1000, respectively. Thus, an increasing trend of grain size with the sintering temperature is shown.

The theoretical saturation magnetization of $\text{Sr}_2\text{FeMoO}_6$ is around $4\mu_B/\text{f.u.}$, which equals 52.88 emu/g, and the ferromagnetism results from a long range ferrimagnetic coupling with Fe–O–Mo orderly arrangement as shown by Monte Carlo simulation [7]. The hysteresis loops of S900, S950 and S1000 are displayed in

Fig. 2. One can see that although M_s increases significantly from 4.0 to 11.0 emu/g with the sintering temperature, it is quite small compared to the reported one at room temperature [4]. The low M_s indicates the existence of disorder in the sample since the crystal structure and the cell parameters are the same as those of the ideal $\text{Sr}_2\text{FeMoO}_6$. Effects of thermal disturbance, size effect, anti-site defects (ASD), anti-phase domains (APD) and intrinsic disorder are believed to be the most probable sources reducing the magnetic moment in double perovskite [5]. ASD results from the exchange of Fe and Mo moments among the B' and B sites of a double perovskite structure. APD originates from two coherent crystallites facing each other with different octahedral B' and B sites but is occupied by similar Fe or Mo atoms forming the planes of either strong antiferromagnetic Fe–O–Fe or weak antiferromagnetic Mo–O–Mo bonds [8–10]. On the other hand, the intrinsic disorder in the lattice structure increases with the sintering temperature. This is indirectly proved by the presence of a magnetic spin glass phase by the ac susceptibility measurement [5]. Besides, for nanoparticles, the broken exchange bonds and the translational symmetry breaking of the lattice at the surface will induce extra disordered spins. All of the disorders lead to decrease of the saturation magnetization and formation of insulator matrix [11,12], which may be used to improve the dielectric loss and reduce the eddy current loss.

Fig. 3 shows the relative complex permeability and permittivity spectra of $\text{Sr}_2\text{FeMoO}_6/\text{epoxy}$ composites. As shown in Fig. 3(a), for all three samples, values of μ' and μ'' change slightly in the range of 2–18 GHz. However, the values of μ'' decrease in the low frequency range and then vary with the increase of frequency for each sample. The variations occurred at different frequencies, which have been marked by black arrows and the changing frequency moves to low value as the sintering temperature increases. It is generally agreed that the permeability spectrum is mainly determined by the natural resonance in the magnetic microwave absorption material [13]. According to the natural resonance equation [14] $2\pi f_r = \gamma H_a$, where γ is the gyromagnetic ratio and $H_a = 4|K_1|/3\mu_0 M_s$, increasing M_s will result in decreasing H_a with the sintering temperature increasing as shown in Fig. 2. Moreover, the lattice defects, interior stress as well as magnetic exchange coupling, etc. resulting from the non-equilibrium $\text{Sr}_2\text{FeMoO}_6$ particles can also induce the extra effective anisotropy field [15–17]. Thus, the effective anisotropy field decreases with temperature increase. As a result, it is reasonable to consider that the natural resonance frequencies for the three samples shift to

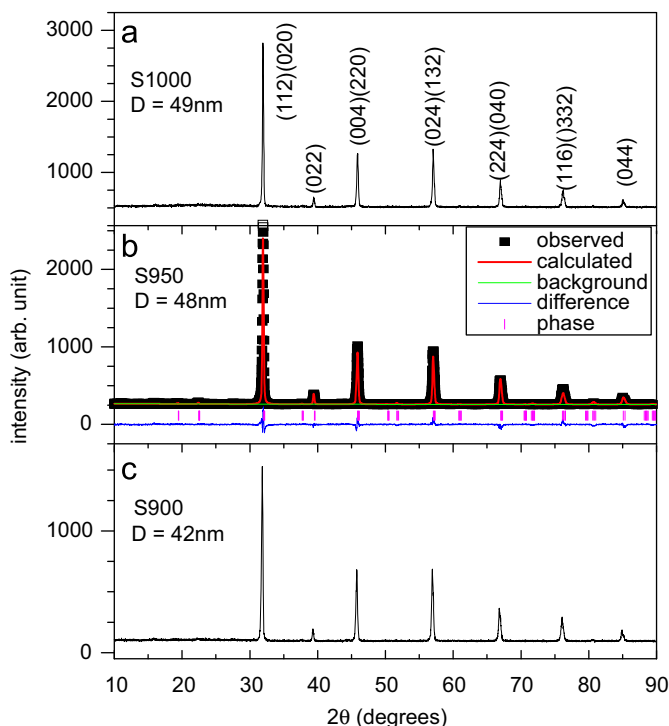


Fig. 1. XRD pattern of S900, S950 and S1000 and the Rietveld refinement of powder XRD data for S950.

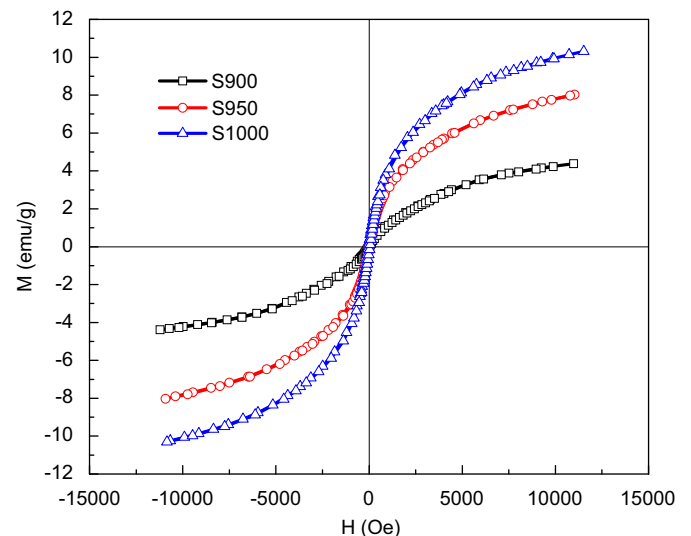


Fig. 2. Magnetic hysteresis loop of S900, S950 and S1000.

Download English Version:

<https://daneshyari.com/en/article/1811108>

Download Persian Version:

<https://daneshyari.com/article/1811108>

[Daneshyari.com](https://daneshyari.com)